NIPPON STEEL TECHNICAL REPORT No. 103 MAY 2013

Technical Report

UDC 621 . 791 . 72 : 629 . 11 . 011 . 5

Current Problems and the Answer Techniques in Welding Technique of Auto Bodies—Second Part

Yasuaki NAITO*
Tatsuya SAKIYAMA
Tetsuro NOSE
Shinji KODAMA
Yasunobu MIYAZAKI

Abstract

Research progress concerning laser welding and mechanical clinching which are being used for the assembly of auto bodies. On the laser welding, usage of remote welding is recently expanding, therefore, the next things were shown: 1) attenuation phenomenon of laser power, as an important point on the remote welding, caused by plume blowing out of workpiece, 2) hybrid spot welding technique applicable for the welding of three steel sheets highly differing in thickness and 3) laser welding method accompanied with filler vibration corresponding to the welding with a gap between steel sheets. Furthermore, as a non-melting joining technique, mechanical clinching was referred to and property of strength concerning one-side riveted joints were introduced.

1. Introduction

The application of laser processing in the automotive industry began with laser cutting of ignition coil paper at GM in 1972.[1)] In 1985, Toyota Motors and Audi started applying lasers to tailored blanks.[2)] At about the same time, GM used lasers for welding the roofs of its cars—the first example of laser application in an assembly process.[3)] Today, with the improvements in laser oscillators, remote welding can be performed utilizing a galvano-mirror to allow for a flexible welding operation within a prescribed three-dimensional space. Remote welding is reported to have been used for the first time in 2003 to weld swing doors at the Chrysler factory. In Japan, the application of remote welding to instrument panel reinforcements at Futaba Industrial[4)] and to trunk lids and hoods at Nissan Motors has been reported.[5)]

However, the essential points of this welding technology are still not completely understood. Indeed, it has only been used in practice for the last 10 years. In this report, we review the results of recent studies that examined how remote welding is affected by the laser-induced plume (hot metal vapor) that blows out from the keyhole during welding. In addition, as an example of the application of remote welding, we describe the hybrid spot welding method for joining three steel sheets having a large thickness ratio. Moreover, when a clearance occurs between two steel sheets, they cannot be joined by laser welding alone. The laser-arc hybrid welding method is used for feeding supplementary molten metal into the weld pool. However, there is a possibility that increased welding deformation results from the large heat input in this method. In order to avoid the increase in welding heat input and to minimize defects due to incomplete fusion of the filler, the filler oscillation laser welding method was developed. This method shall also be described in this report.

In recent years we have seen an increase in the use of multimaterial structures in car bodies. When joining a steel sheet and an aluminum sheet, the mechanical method of riveting is commonly used. The joining of such dissimilar metals shall be described in a separate report. In this report, we discuss the possibility of rivet joining

* Senior Researcher, Dr.Eng., Welding & Joining Research Center, Steel Research Laboratories
20-1 Shintomi, Futtsu, Chiba 293-8511

of steel sheets from the viewpoint of joint strength.

2. Laser Welding

2.1 Attenuation of laser power in plumes

Remote laser welding is now being applied in actual production processes. As the beam source, a carbon dioxide gas laser or a solid-state laser can be used. In laser welding operations that use a carbon dioxide gas laser with a wavelength of 10.6 μm, the laser-induced plume blowing out from the keyhole in plasma state absorbs the laser energy through inverse bremsstrahlung, reducing the laser power significantly before it reaches the workpiece.[6] In the past, it was thought that the laser induced plume would not affect the laser welding with solid-state lasers because these lasers with a wavelength of approximately 1 μm (e.g., the fiber laser) are not affected by inverse bremsstrahlung. In recent years, however, as the quality of the solid-state laser has improved, the condenser lens can be set apart from the work, revealing that, even in these lasers, the laser beam is refracted and the laser power is attenuated in the plume.[7, 8] In order to implement remote welding on a stable basis, it is necessary to have a thorough understanding of the above phenomena. Therefore, in our study we aimed to quantitatively determine the shift of the focal point and the attenuation coefficient of laser beam caused in the plume during welding.

2.1.1 Change in penetration caused by the plume

In welding operations using a solid-state laser, it is common practice to use an air knife in order to prevent the protective glass from being stained by spatters and fumes from the work (**Fig. 1**). Unless a side- or center-shielded nozzle is used, the plume from the work spreads freely until it is intercepted by the air knife. The image of a weld bead obtained when the air knife was set at a height of 210 mm from the specimen is shown in **Fig. 2** (a). The beam source used was a fiber laser. A 3 kW laser beam was condensed to a spot 0.92 mm in diameter at a focal length of 460 mm for a melt run at 1 m/min. Although the front bead is uniform as a whole, the state of oxidization of the back bead varies along the length of the bead, suggesting that the condition of penetration differs according to the welding point. Fig. 2 (b) shows photographs of weld cross sections and plumes at various distances from the weld start point. The penetration is shallow where the plume rises high and deep where the plume was low.

2.1.2 Relationship between plume height and cross-section area of the fusion

The relationship between the height of the plume and the cross-section area of the fusion (weld metal) was obtained from melt runs

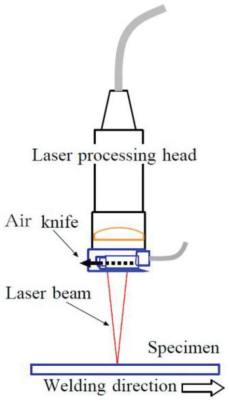

Fig. 1 Configuration of air knife at welding

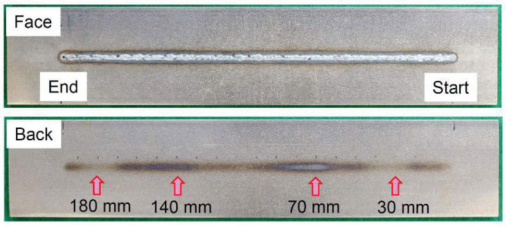

(a) Appearance of welded specimen

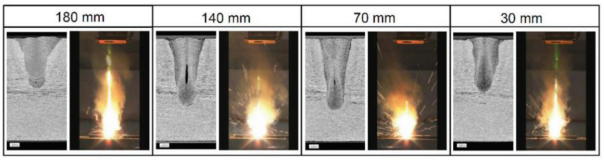

(b) Photos of plume and penetration at that plume state

Fig. 2 State of plume and penetration

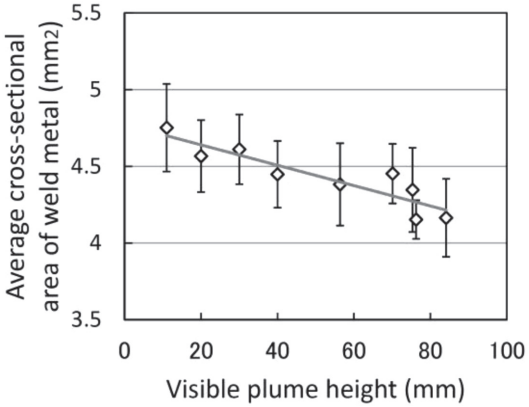

Fig. 3 Dependence of weld area on plume height

in which the plume height was varied by using an air knife.[8] The relationship obtained is shown in **Fig. 3**. In the experiment using a YAG laser, a 4 kW laser beam was condensed to a spot 0.84 mm in diameter at a focal length of 280 mm and the melt runs were performed at a welding speed of 2 m/min. During the melt run, the maximum height of the air knife was limited to 160 mm to prevent excessive variations in the plume height and to stabilize the penetration. Since the experiment did not involve any factor that would change the efficiency of fusion, the efficiency was considered constant. Therefore, the cross-section area of fusion is considered to be proportional to the energy that is absorbed in the workpiece. Namely, Fig. 3 shows that as the plume rises higher, the energy that reaches the work is attenuated proportionally.

2.1.3 Attenuation coefficient of laser beam in the plume

With the air knife height set to 20 mm and the plume height kept constant, a melt run was carried out while varying the laser output to obtain the relationship between the cross-section area of fusion and the laser output. The relationship obtained is shown in **Fig. 4**. In the experiment, the cross-section area of fusion was proportional to the laser output and the following equation was obtained.

$$\text{Area (mm}^2\text{)} = 7.636 \times \text{relative power} - 3.074 \quad (1)$$

By using the above relationship, the laser power can be calculated from the cross-section area of fusion shown in Fig. 3. The calculated laser power is considered to be equivalent to the laser power

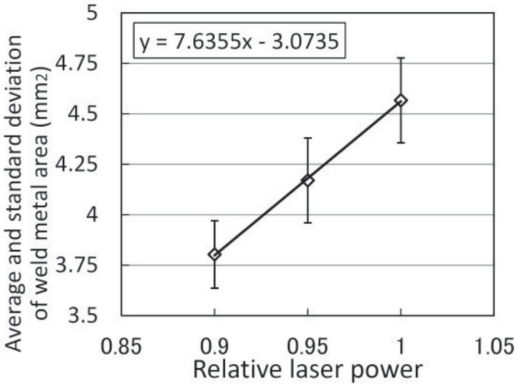

Fig. 4 Dependence of weld area on laser power

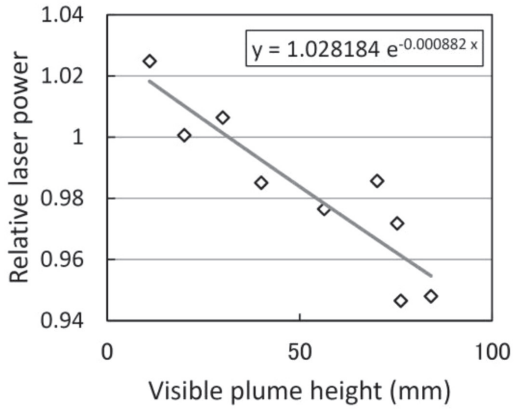

Fig. 5 Dependence of relative laser power at work on plume height

that reached the steel sheet while being attenuated by the plume. **Fig. 5** shows the relationship between the plume height and the laser power that reached the steel sheet. Equation (2) was obtained by regression under the assumption that the laser beam was attenuated at a constant rate per unit length of the plume that it passed through. In general, we can use the approximation of the following equation (3) that expresses a linear relationship between the relative laser power and the visible plume height. Thus, it was estimated that when the laser beam passes through the visible plume over a distance of 100 mm it is attenuated 8.8%.

Relative laser power

$= 1.028 * \exp(-0.000882 \times \text{plume height (mm)})$ (2)

$= 1.028 * (1 - 0.000882 \times \text{plume height (mm)})$ (3)

The attenuation of the laser beam by the plume can be attributed to Rayleigh scattering.[9] On the other hand, the focal point shift caused by the plume can also influence the penetration.[10] However, when the height of the air knife from the steel sheet surface is small as in the present experiment, it is estimated that the focal point shift is so small that its effect on the penetration is insignificant.[11] Nevertheless, when the height of the air knife is substantially large as in remote welding, we consider it necessary to pay due attention to the effect of the focal point shift.

2.2 Hybrid spot welding

As mentioned in Part I of the report,[12] car body manufacturing involves the production of a number of parts, which require welding of three steel sheets having a large thickness ratio. In the spot welding of those parts, there is difficulty in forming stable nuggets between the thin and thick steel sheets. Here, we present the results of our study [13, 14] on a technique to weld three steel sheets successfully by applying remote laser welding from the thin steel sheet side to form a weld between the thin steel sheet and the thick steel sheet after spot welding of the thin and thick steel sheets.

We used the following combination of three steel sheets having a large thickness ratio: one 0.8 mm-thick galvannealed (GA) steel sheet of 270 MPa class and two 2.3 mm-thick GA steel sheets of 590 MPa class. The steel sheet arrangement we studied was 0.8 mm + 2.3 mm + 2.3 mm (thickness ratio: 6.75). Each of the steel sheets had been coated on both sides (coating weight: 45 g/m^2). For resistance spot welding, a servomotor-driven, single-phase, AC spot welding machine was used. The electrode used was a Cr-Cu electrode of DR type (tip radius of curvature: 40 mm, tip diameter: 6 mm).

The welding conditions were as follows: electrode force 2.45 kN and welding time 29 cycles. After spot welding, laser welding was performed from the thin steel sheet side, with the laser welded diameter controlled between 4.5 to 7.5 mm (set value), and the soundness of the weld beads was examined. As the beam source, a fiber laser was used. It was condensed to a 0.6-mm spot at a focal distance of 600 mm for remote welding. The laser welding conditions were such that the laser beam passed through the first thin steel sheet (0.8 mm), but did not completely pass through the second thick steel sheet. Namely, the conditions were as follows: laser power 2 kW, welding speed 4 m/min, and defocus distance +3 mm (hereafter called the 2 kW conditions) or laser power 2.5 kW, welding speed 4 m/min, and defocus distance +6 mm (hereafter called the 2.5 kW conditions).

In **Fig. 6**, macro-photographs of nugget cross-sections show the dependence of nugget formation on the welding current. **Fig. 7** shows a sound bead formed by remote laser welding performed under 2 kW conditions after spot welding and a defective bead caused by the blow-off of the molten metal during remote laser welding. Regardless of the nugget diameter, as the remote welding diameter was increased, the molten metal was blown off, preventing the formation of sound beads. **Fig. 8** shows the measured diameters of nuggets formed by spot welding between the two thick steel sheets and between the thin and thick steel sheets and the results of our study on whether sound weld beads could be formed by remote

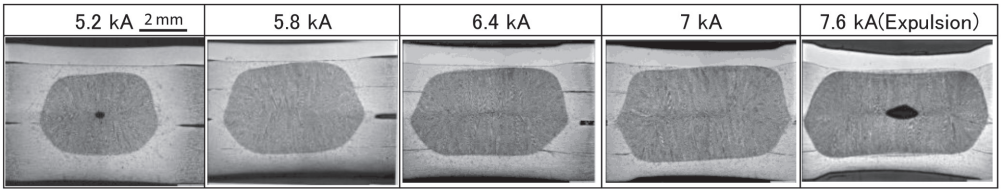

Fig. 6 Dependence of nugget formation on welding current (sheet combination: 0.8 mmt / 2.3 mmt / 2.3 mmt)

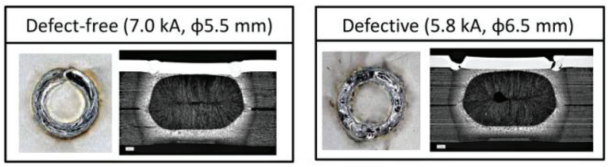

Fig. 7 Surface appearance and macro cross-sections without and with defect in hybrid spot welding

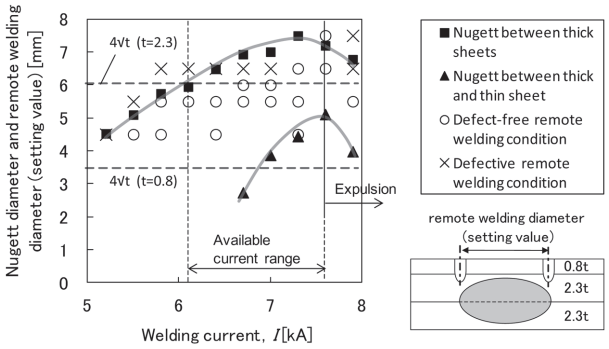

Fig. 8 Weldability lobe of spot and remote welding for three galvannealed steel sheets. (sheet combination: 0.8 mmt + 2.3 mmt + 2.3 mmt)

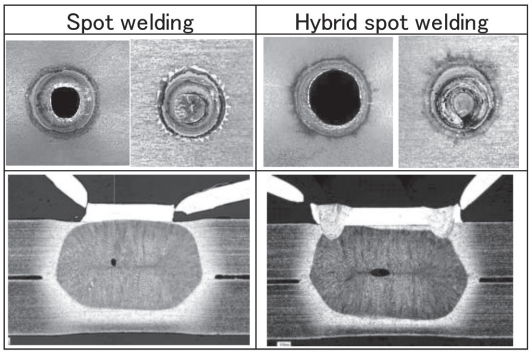

Fig. 9 Surface appearance and macro cross-sections of spot and hybrid spot weld after cross tensile test (welding current 6.1 kA)

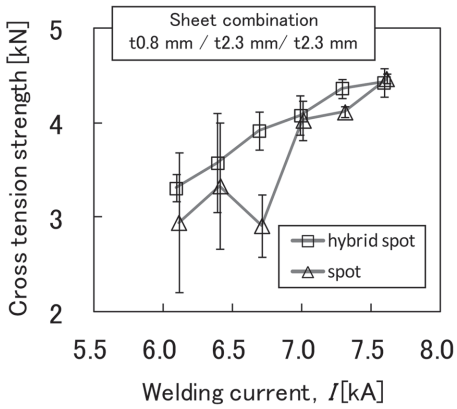

Fig. 10 Comparison of cross tension strengths between thin and thick sheets of spot welded joints and hybrid spot welded joints

welding. Assuming that the proper current range in spot welding in terms of the nugget diameter is between $4\sqrt{t}$ (t: sheet thickness) and the diameter at which an expulsion occurs, nuggets $4\sqrt{t}$ or more in diameter could be formed between the two thick steel sheets within the current range of 6.1 - 7.6 kA, whereas between the thin and thick steel sheets, the proper current range for the formation of nuggets of comparable size was narrower –7.0 to 7.6 kA.

On the other hand, in remote laser welding, we found that as long as the laser welding diameter was almost equal to or less than the diameter of the nuggets formed between the two thick steel sheets, sound welds could be formed between the thin and thick steel sheets. Ordinarily, in lap laser welding of GA steel sheets, unless a clearance is provided between the steel sheets, sound beads cannot be formed because the molten metal is blown off by zinc vapor. Using the hybrid spot welding method described above, however, it is possible to form sound beads even when there is no clearance between the steel sheets, as shown in Fig. 7. The reason for this is that the coated metal is mostly removed from the solid-state bonded area between the thin and thick steel sheets during spot welding.

In order to evaluate the strength of the welded joints, cross-tension test specimens were prepared by spot welding and hybrid welding. For spot welding, the current value was used as a parameter, and remote welding was performed under the 2.5 kW conditions with a welding diameter of 4.5 mm. The specimen shape was in accordance with JIS Z 3137. As the third steel sheet, a 45 mm-square steel sheet was used. In the cross-tension test, the first thin steel sheet (GA steel sheet of 270 MPa class) was peeled from the second thick steel sheet (GA steel sheet of 590 MPa class) at a tension speed of 10 mm/min. **Fig. 9** shows the appearance of fractured welded joints and macro cross sections of the joints after the test, and **Fig. 10** shows the cross-tension strength (CTS) of the welded joints. The error bars indicate the high and low limits of the joint strength, and symbols □ and △ indicate the average values. In spot welding, CTS varied widely in the welding current range of 6.1 - 6.7 kA. When the welding current was increased to 7.0 kA or more, the variation narrowed down and the CTS improved. We believe this could be explained as follows. While the solid-state bonded area formed between the thin and thick steel sheets in the low welding current range was imperfect, stable corona was formed when the welding current was 7.0 kA or more.

In hybrid welding, with the increase in welding current, the CTS of the welded joints increased. When the welding current was increased to 7.0 kA or more, CTS became nearly the same as that obtained by spot welding. The variation in CTS in the current range of 6.1 - 6.7 kA was narrower than that in the spot welding and the average CTS was higher. This may be explained as follows. As can be seen from the fact that the fracture in the macro cross section is located around the weld metal (Fig. 9), welds of a certain diameter were formed by remote welding and thereby the low limit of CTS was guaranteed. Similar results were obtained by tensile shear test; hence, it may be said that hybrid spot welding is effective in enhancing the CTS of welded joints and narrowing down its variation in the low welding current range.

2.3 Filler oscillation laser welding

2.3.1 Fusion welding of lap joints

Laser welding is a welding method that features low heat input and low strain. On the other hand, since this method uses a comparatively small amount of molten metal, irregular joints commonly occur when there is a clearance between the steel sheets to be weld-

ed together. It is possible to increase the allowance for clearance by supplying a filler wire ("filler") during the welding. However, since the laser is a very small heat source, irregular beads can occur unless the filler is fed precisely. In order to keep the filler in a stable melting condition, we tested the filler oscillation method in which the filler is fed to the weld while being kept oscillating at a high frequency.[15)]

A schematic of the filler oscillation laser welding method is shown in **Fig. 11**. The filler that is set ahead of the laser beam in the welding direction is oscillated at the prescribed frequency and amplitude. The oscillator that converts the rotary motion of the motor into the reciprocal motion of the filler is capable of high-speed oscillations up to 50 Hz.

Fig. 12 shows specimens welded using this method with varying oscillation frequency and amplitude. When the oscillation frequency was low (20 Hz or less), the beads meandered and the bead ends became uneven. With a high oscillation amplitude, the filler showed a tendency to remain unmelted. On the other hand, when the oscillation frequency was increased to 30 Hz, good beads could be obtained at all the oscillation amplitudes tested. When the oscillation amplitude is increased, the filler traveling speed relative to the laser beam increases. Hence, the heat input to the filler per oscillation would decrease, causing the amount of filler fed to the steel sheets to decrease, displaying a periodical change in bead shape. The heat input to the filler per oscillation also decreases when the oscillation frequency is increased. In this case, however, uniform beads can form since the molten filler is fed more frequently (i.e., the filler is fed almost continuously). On the basis of the above findings, we adopted a high-speed oscillation (oscillation frequency: 40 Hz) in the subsequent study.

Fig. 13 shows the dependence of the penetration shape on the clearance between the steel sheets. The penetration shapes shown were obtained by three methods: laser welding alone, laser welding with fixed filler, and laser welding with oscillating filler. The specimens used were 1.2-mm-thick GA steel sheets, and the filler was a 1.2-mm-diameter filler wire for welding (JIS Z 3312 YGW12). When the clearance between the steel sheets was 0.6 mm, the weld was separated in case of laser welding without filler. However, when

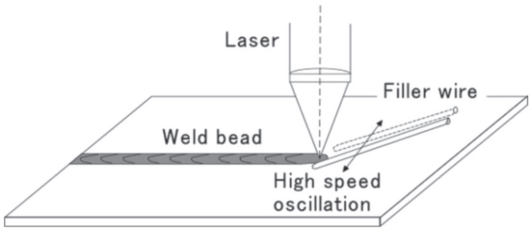

Fig. 11 Schematic illustration of filler wire oscillation laser welding

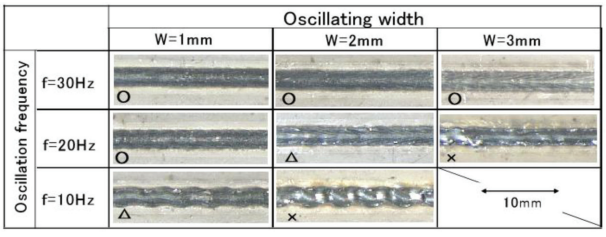

Fig. 12 Dependence of weld bead appearance on oscillation condition

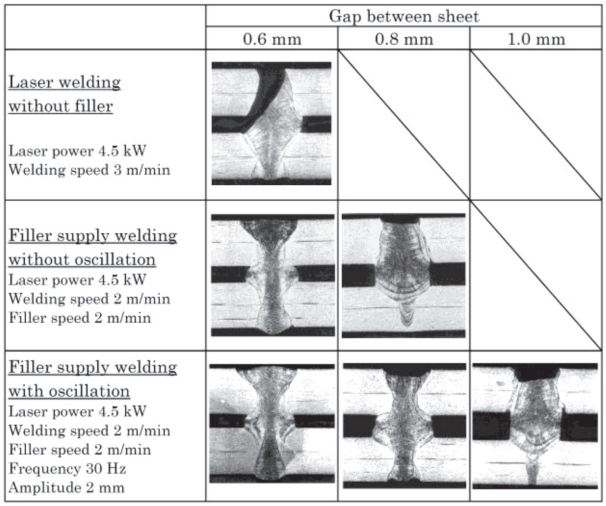

Fig. 13 Dependence of penetration shape on sheet gap in lap joint

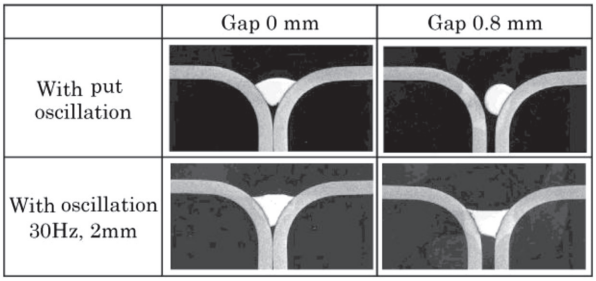

Fig. 14 Cross sections of laser brazed joints

the filler was used, it became possible to secure an adequate amount of molten metal, and hence a good penetration shape was obtained. When the clearance was 0.8 mm, the lower steel sheet could not be penetrated without an oscillating filler. By oscillating the filler, however, a good penetration shape through the lower steel sheet was obtained, although a slight degree of under-filling occurred. We explain this as follows. Without filler oscillations, the molten filler filled the gap between the steel sheets, thereby preventing the full penetration welding . When the filler was oscillated, however, the irradiation of the laser and the supply of molten metal were repeated periodically, thereby offering a good penetration shape.

2.3.2 Brazing of flare groove welded joints

Fig. 14 shows an example of an application of filler oscillation in laser brazing. A [Cu + 3%Si] filler was applied to flare groove welded joints of 0.8-mm-thick GA steel sheet. The laser output was 3 kW, the welding speed was 2 m/min, and the condensed beam diameter was 2.3 mm. Without filler oscillations, the brazed parts became convex in shape and the brazing material adhered only to one of the two steel sheets when the clearance between the steel sheets was 0.8 mm. On the other hand, it was confirmed that when the filler was oscillated, the profile of the brazed part became flat and the allowance for clearance increased.

3. One-Side Riveting

As shown in Fig. 1 in Part I,[12)] the peel strength (CTS) of spot-welded joints of high-strength steel sheets decreases when the steel sheet strength is 780 MPa or more. Here we evaluated the depen-

dence of the strength of the blind-riveted joints on the strength of the steel sheets[16] and studied the possibility of improving the strength of the joints of the high-strength steel sheets by using blind riveting. Blind riveting is a joining method in which the steel sheets to be joined together are predrilled with through holes, so that rivets can be driven into the steel sheets through the holes from one side to the other.

We used steel sheets with a thickness of 1.2 - 2.0 mm and a tensile strength of 270 - 1,470 MPa. All the steel sheets were predrilled with through holes. The two steel sheets of each pair were placed one on top of the other with the holes aligned accurately. Then, they were joined together using Infastech rivets (**Fig. 15**). The rivet sleeve diameter was 6.8 mm and the diameter of the holes drilled in the steel sheets was 7.1 mm. In order to evaluate the static strength of the riveted joints, we carried out a tensile shear test and a cross-tension test using JIS Z 3136/3137 specimens. In addition, an L-tension test was carried out by using 30-mm-wide L-shaped specimens. The length of the bent section (corresponds to the flange of the member) was 30 mm and the distance between the flange end and the rivet center was 15 mm. The tension speed was kept constant at 20 mm/min during the tensile shear test and the L-tension test and 10 mm/min during the cross-tension test.

Fig. 16 shows the tensile shear strength (TSS) of the blind-riveted joints. The TSS increased as the steel sheet strength increased. With a thick high-strength steel sheet (sheet thickness: 1.6 mm), however, TSS tended to become saturated as the steel sheet strength increased. For a 1.2-mm-thick steel sheet, the mode of fracture was a rivet slip-out (i.e., the rivet slipped out as a result of steel sheet deformation around the drilled hole). In the case of 980 MPa and 1,470 MPa steel sheets with a thickness of 1.6 mm or more, the fractures occurred at the rivet center. For the joints of 1.2-mm-thick steel sheets and the sheets of 590 MPa or less, a rotational defomation occurred around the weld during the tensile shear test. As a result, a component of force in the peel direction was produced. At the same time, steel sheet deformation occurred around the drilled hole. This is considered to be the mechanism that eventually caused the rivet slip-out mentioned above. Since the steel sheet deformation around the drilled hole determined the joint strength, we believe that the joint tensile strength increased with the increase in steel sheet strength. On the other hand, we estimated that when the steel sheet is thick and strong, the centrifugal distortion is restrained and the component of the force in the peel direction in the joints of the thick high-strength steel sheets is not very high. Moreover, because the steel sheet strength around the drilled hole was high, the shear stress acting on the rivet center reached the critical stress for the rivet, causing the fracture mentioned above. This explains why the tensile strength of the joints of the high-strength steel sheets showed a tendency to become saturated against the increase in steel sheet strength.

Fig. 17 shows the CTS of the blind-riveted joints. It was confirmed that unlike the joints obtained by resistance spot welding, the CTS of blind-riveted joints did not decrease even when the steel sheet strength exceeded 590 MPa, and that the CTS continued increasing until the steel sheet strength reached 1,470 MPa. The mode of fracture was a rivet slip-out, not a fracture at the rivet center.

Fig. 18 shows the L-shape tension strength (LTS) of the riveted joints. Like CTS, LTS continued increasing until the steel sheet strength reached 1,470 MPa, with the LTS value being about one-half that of CTS. As in the cross-tension test, the mode of fracture was a rivet slip-out and only the edge of the drilled hole was partly deformed. Thus, in the case of L-shaped joints, because the stress is concentrated around a certain part of the edge of the drilled hole, LTS decreased more than CTS.

Next, we studied the dependence of LTS on the distance between the blind rivet center and the flange end.[17] This distance varied from 5 mm to 15 mm. **Fig. 19** shows the LTS of the blind-riveted joints.

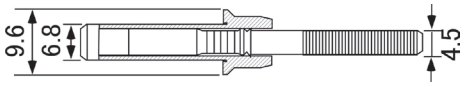

Fig. 15 Schematic illustration of blind-rivet

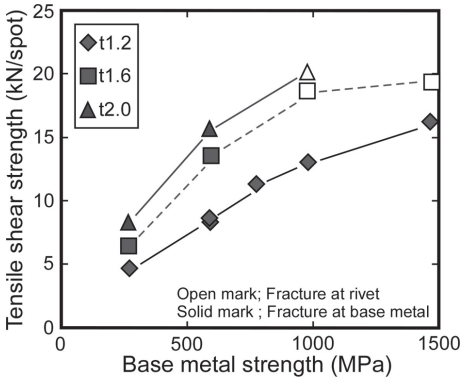

Fig. 16 Dependence of tensile shear strength on base metal strength

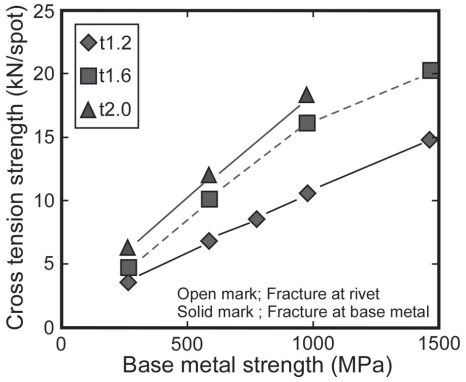

Fig. 17 Dependence of cross tension strength on base metal strength

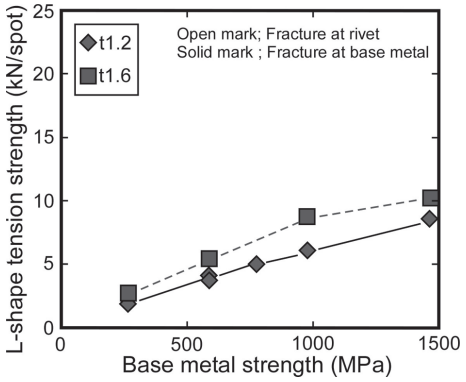

Fig. 18 Dependence of L-shape tension strength on base metal strength

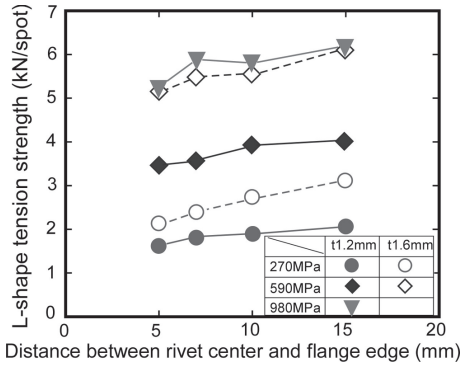

Fig. 19 Dependence of L-shaped tension strength on distance between rivet center and flange edge

When the distance between the rivet center and the flange end was between 10 mm and 15 mm, the LTS of all specimens was very close. However, when the distance was less than 10 mm, LTS decreased as the distance was shortened. The mode of fracture in all the cases was a rivet slip-out regardless of the distance between the rivet center and the flange end. We did not observe any fracture at the rivet. We believe that when the said distance is shortened, the part that supports the load outside the rivet narrows down, causing the edge of the drilled hole to be deformed easily and LTS to decline. With the shortening of the distance, the riveted joints of the 270 MPa steel sheets show a higher rate of decline in LTS than those of the other steel sheets. This may be because steel sheets having comparatively low strength tend to be deformed easily around the drilled holes.

4. Conclusions

"Securing safety and improving fuel efficiency" has long been an important challenge in the automotive industry. At the same time, the automotive industry is continuously endeavoring to offer a more comfortable ride and a more sophisticated car design. In order to meet these multiple requirements, high-strength steels of 980 MPa or more have been increasingly utilized. Under those conditions, innovations in car manufacturing technology, including joining techniques, are strongly required. We would like to support the development of reliable new joining techniques through further improvements in the existing techniques that were described here and in Part I of the report.

References

1) Kutsuna, M.: Welding Technology. 50 (5), 127 (2002)
2) Natsumi, F.: Press Working. 34 (8), 18 (1996)
3) Larsson, J. K.: Welding Technology. 51 (11), 86 (2003)
4) Sanpei, K.: Journal of Japan Laser Processing Society. 16 (1), 8 (2009)
5) Tarui, D., Mori, K., Yoshikawa, N., Hasegawa, T.: Proceedings of the 68th Laser Materials Processing Conference. 157 (2007)
6) Ono, M., Nakada, K., Kosuge, N.: Quarterly Journal of the Japan Welding Society. 10 (2), 239 (1992)
7) Kawato, Y., Kinoshita, K., Katayama, S., Tsubota, Y., Ishide, T.: Journal of Japan Laser Processing Society. 13 (1), 41 (2006)
8) Miyazaki, Y., Katayama, S.: Preprints of the National Meeting of J.W.S. 90, 208 (2012)
9) Kawato, Y., Kinoshita, K., Matsumoto, N., Mizutani, M., Katayama, S.: Quarterly Journal of the Japan Welding Society. 25 (3), 461 (2007)
10) Oiwa, S., Mizutani, M., Kawato, Y., Katayama, S., Ozawa, N.: Preprints of the National Meeting of J.W.S. 83, 226 (2008)
11) Miyazaki, Y., Katayama, S.: Preprints of the National Meeting of J.W.S. 87, 376 (2010)
12) Furusako, S., Watanabe, F., Murayama, G., Hamatani, H., Oikawa, H., Takahashi, Y., Nose, T.: Shinnittetsu Giho. (393), 69-75 (2012)
13) Naito, Y., Murayama, G., Miyazaki, Y.: Preprints of the National Meeting of J.W.S. 88, 152-153 (2011)
14) Naito, Y., Murayama, G., Miyazaki, Y.: Preprints of the National Meeting of J.W.S. 89, 52-53 (2011)
15) Kodama, S., Miyazaki, Y.: Welding Guide Book 6, the Japan Welding Society, "Development in Advanced Welding Processes". 2008, p. 175
16) Sakiyama, T., Miyazaki, Y.: Preprints of the National Meeting of J.W.S. 89, 58 (2011)
17) Sakiyama, T., Miyazaki, Y.: Preprints of the National Meeting of J.W.S. 90, 234 (2012)

Yasuaki NAITO
Senior Researcher, Dr.Eng.
Welding & Joining Research Center
Steel Research Laboratories
20-1 Shintomi, Futtsu, Chiba 293-8511

Shinnji KODAMA
Senior Researcher
Welding & Joining Research Center
Steel Research Laboratories

Tatsuya SAKIYAMA
Senior Researcher
Welding & Joining Research Center
Steel Research Laboratories

Yasunobu MIYAZAKI
Chief Researcher
Welding & Joining Research Center
Steel Research Laboratories

Tetsuro NOSE
General Manager, Dr.Eng.
Welding & Joining Research Center
Steel Research Laboratories